*Proc. 14th Int. Conf. on Muon Spin Rotation, Relaxation and Resonance (μSR2017)*
JPS Conf. Proc. **21**, 011050 (2018)
https://doi.org/10.7566/JPSCP.21.011050

# New Capabilities at Pulsed Muon Facilities with Pulsed Radio-Frequency Techniques

Stephen P. COTTRELL[1*] and Sean R. GIBLIN[2]

[1]*ISIS Facility, STFC - Rutherford Appleton Laboratory, Harwell Campus, Didcot, Oxfordshire, OX11 0QX, UK*
[2]*School of Physics and Astronomy, Cardiff University, Cardiff, CF24 3AA, UK*

**E-mail: stephen.cottrell@stfc.ac.uk*

(Received June 25, 2017)

At a pulsed muon source, a radio-frequency pulse timed to rotate the implanted muon spin polarization by 90° can be used to completely remove the frequency limitations imposed on conventional spin rotation experiments by the finite muon pulse width. This contribution presents two applications of the method, where controlling the excitation bandwidth of the radio-frequency pulse provides unique information. In the first case, an intense 90° pulse is used for broadband excitation of a paramagnetic system, while in the second case a low power pulse applied in the presence of a field gradient excites a limited frequency band leading to spatial localization of the muon signal.

**KEYWORDS:** radio-frequency, pulsed techniques, pulsed muon source, imaging

## 1. Introduction

At pulsed muon sources, pulsed radio-frequency (RF) techniques can be used to greatly enhance the scope of possible measurements. At its simplest, a 90° RF pulse can be used to completely remove the frequency limitations imposed on conventional spin rotation experiments by the finite muon pulse width [1], and at ISIS additional detector banks are planned (initially on the HiFi spectrometer) to better exploit this capability. More complex pulsed RF sequences are, however, possible despite the short muon lifetime, and a number of sequences have been adapted from NMR, demonstrated and used to good effect in μSR experiments [2-5]. For much of this work, the pulsed structure of the source is vital; this allows the use of very high instantaneous powers with minimal RF heating, while enabling time differential data to be measured to long times at high counting rates and with minimal background.

This contribution focusses on two examples that make use of a simple 90° RF pulse, where the pulse excitation bandwidth is important to the measurement results. In the first case, broadband excitation of a paramagnetic system is demonstrated for a high power 90° pulse by following the signal amplitudes of the $\nu_{12}$ and $\nu_{23}$ resonance lines of muonium formed in quartz as a function of resonance offset. In contrast, in a second example, spatial localization of the muon signal is achieved by applying a low power 90° pulse in the presence of a static field gradient. The method is demonstrated by reconstructing a rudimentary image using a selective irradiation process [6]. All experiments were carried out using the EMU spectrometer [7] at the ISIS muon source.

## 2. Broadband Pulse Excitation - Extending Spin Rotation Measurements

The aim of the first example was to examine how high power pulsed RF techniques might be used for measurements akin to Fourier Transform NMR, simultaneously exciting multiple transitions with all the advantages of enhanced signal to noise (compared to continuous wave excitation). The potential for this type of measurement was recently highlighted by work by Spindler et al [8], where EPR pulses of width ~20ns were applied to create a broadband excitation of ~100MHz.

An RF coil consisting of approximately four turns of 24 swg Cu wire was wound to provide an access volume sufficient for the 25x25x2mm fused quartz plate used as the test sample. The coil was tuned and matched to 50Ω at a working frequency of 79.32MHz, a series resistor being added to spoil the Q of the coil to obtain fast RF rise/fall times.

Free precession signals were recorded for muonium formed in the quartz sample following a 60ns RF pulse, a pulse length determined to give an approximate 90° spin rotation of the muon spin. Both the $\nu_{12}$ and $\nu_{23}$ transitions associated with the triplet state [10] are excited, the response being explored as a function of resonance offset. With the static field set such that both frequencies fall close to that of the RF carrier, both transitions are excited and recorded with approximately equal weight; this case is shown in Fig. 1(a). As the field is adjusted to move transition frequencies away from the carrier frequency, excitation will depend on the spectral width of the RF pulse, and the two transitions may no longer be excited with equal weight; this case is shown in Fig. 1(b). A plot of the amplitude of the $\nu_{23}$ line (obtained by fitting in the time domain) as a function of field is shown in Fig. 1(c); the dashed vertical (blue) line indicates the RF carrier frequency and the red curve is a best fit to a Gaussian lineshape

An excitation bandwidth of ~17MHz would be anticipated for an exact rectangular 60ns RF pulse; however, in practice, the finite rise/fall time of the pulse introduces uncertainties into this value. From fits to the data shown in Fig. 1(c), a FWHM of 13.3(2.5)MHz is obtained. With due regard to pulse imperfections, the data clearly demonstrates the feasibility of using an extended excitation bandwidth in experiments, and shows the bandwidth to be commensurate with the pulse length being used for the test.

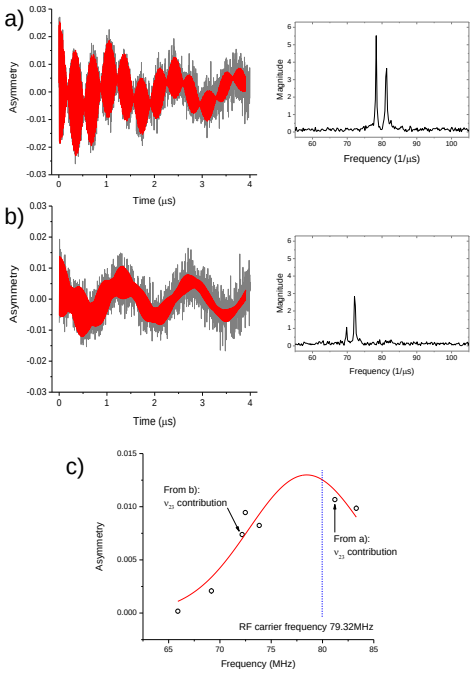


**Fig. 1.** Signal from muonium formed in fused quartz, following a 60ns 90° RF pulse with a carrier frequency of 79.32MHz, at a static field of 57.1G (a) and 50.5G (b), shown with corresponding Fourier spectra. Both $\nu_{12}$ and $\nu_{23}$ transitions are excited. Amplitude of the $\nu_{23}$ line as a function of resonance offset from the fixed carrier (c), the frequency being adjusted by varying the static field.

## 3. Narrowband Pulse Excitation – Localizing the μSR signal

In contrast to the first example, the second presents an application of a low power 90° RF pulse, demonstrating that spatial localization of the muon signal can be achieved if the pulse is applied in the presence of a static field gradient. In this case, because of the narrow spectral width of the RF pulse, the muon signal is localized to a sensitive slice perpendicular to the field gradient [6], with the amplitude and relaxation defined by muon spin density and couplings within that slice.

A NdFeB permanent magnet was orientated such that the field lines, $B_{0z}$, were parallel to the incident muon beam. The field on the pole face of the magnet was ~0.5T, with a field gradient, $G_z$, ~100G.mm$^{-1}$. The RF field was setup by a surface coil wound from 24 swg Cu wire on a plain matrix board and mounted on the pole face of the magnet. These coils provide a similar RF field strength to flattened solenoids typically used for muon measurements, but with much improved field homogeneity ($\Delta B_1/B_1 \sim 5\%$ compared to ~60% for a flattened solenoid). Furthermore, since the sample is in front of the coil, the geometry is better suited to beamline measurements. This setup is similar to that used for the unilateral NMR experiments described in reference 11.

A suitable test sample (shown in Fig. 2(a)) was designed to create a spatially inhomogeneous muon stopping distribution perpendicular to the face of the magnet and surface coil, the stopping distribution being modelled using the SRIM software package [12] (Fig. 2(b)). Muons pass through a Ti degrader (~108mg.cm$^{-2}$) and are stopped in the distinct polythene components, separated by the ~1.4mm air gap, with ~100% diamagnetic fraction.

Muon resonance signals can be localized in the z-direction at a position defined by the RF carrier frequency, ω, as:

$$z = \omega / \gamma_\mu G_z ,$$

and a sensitive slice formed. Signal amplitude follows the muon spin density, as determined by the stopping profile.

A rudimentary image can be constructed by recording the amplitude of the diamagnetic signal following a 90° RF pulse (fitted as a simple exponential decay) as a function of the RF carrier frequency, shown in Fig. 2(c). In this case, an RF field strength of ~5G was used, corresponding to a 90° pulse length of ~3.5μs. This gave an image with a spatial resolution, Δz, of ~50μm. With this setup, there is no spatial localization in the plane parallel to the magnet pole face, although this might be added in a future development.

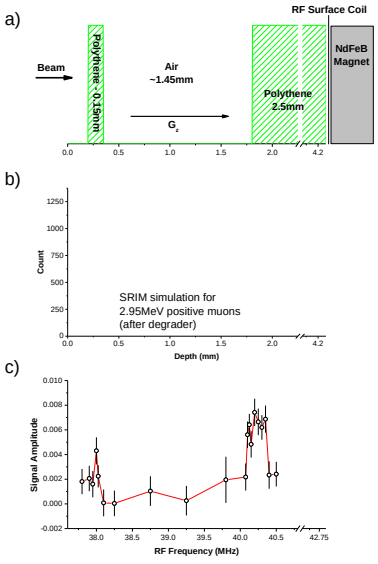


**Fig. 2.** Muons are implanted in a test sample (a) in the presence of a static field gradient ~100G.mm$^{-1}$, with a stopping distribution following the Ti degrader determined from SRIM simulations shown in (b). Signals are recorded following a 3.5μs RF pulse; a sweep of the RF carrier frequency allows a rudimentary image to be reconstructed (c).

## 4. Discussion

The two examples presented in this paper amply demonstrate that even a simple 90° RF pulse can be used very effectively at a pulsed muon source, not only to remove the frequency limitations inherent to this type of facility, but also to provide unique information that couldn't readily be obtained from conventional spin rotation measurements. In this case, the possibility of controlling the pulse excitation bandwidth has been explored.

The potential for applying a high power 90° RF pulse to excite a broad spectral bandwidth, to simultaneously excite and study multiple transitions, is demonstrated by the first example, where a 60ns RF pulse is shown to excite a bandwidth in excess of 13MHz. This has been achieved without any particular optimization, and a combination of shaped RF pulses [8] together with coils optimized at the working frequency should allow at least an order of magnitude improvement in the available spectral bandwidth. It can be envisaged that this method will become a standard tool at pulsed muon sources in the near future, offering the user community a novel method for a new type of measurement.

In contrast, the reconstruction of an image using a low power 90° RF pulse is technically very challenging, and further development would certainly be required before routine application could be considered. However, the success of this example perhaps points the way towards a more general consideration of magnetic resonance imaging methods [13] for muon experiments. Previously this area has received little attention – Kaplan et al. [14] used projection-reconstruction to form a two dimensional image of a target, while Shiroka et al. [15] studied the range and straggle of muons stopped in metal targets. Neither experiment, however, used RF techniques, both instead measuring spin rotation signals with a static field gradient imposed on the applied transverse field to obtain spatial discrimination.

The success of the second example also provides a motivation for exploring other applications that might exploit restricted bandwidth RF pulses. While low power RF pulses inevitably lead to longer than ideal pulse lengths (referenced against the muon lifetime), this disadvantage is largely overcome by the step-change in intensity of current pulsed muon sources. Finally, this work also considered the benefits of surface coils for general application in RF muon measurements. The geometry of these coils is particularly suited to beamline measurements, and results demonstrate that sufficiently large RF fields with comparatively good homogeneity (compared to the usual flattened solenoids) can readily be produced. Furthermore, compared to many other coil designs, spurious signals associated with muons stopping in the coil winding or former are greatly reduced.

## References

[1] S.P. Cottrell, C.A. Scott and B. Hitti, Hyperfine Interact **106**, 251 (1997).
[2] S.R. Kreitzman, Hyperfine Interact **65**, 1055 (1990).
[3] S.P. Cottrell, S.F.J. Cox, C.A. Scott, J.S. Lord, Physica B **289-290**, 693 (2000).
[4] N.J. Clayden, S.P. Cottrell, Phys. Chem. Chem. Phys. **8**, 3094 (2006).
[5] N.J. Clayden, S.P. Cottrell and I. McKenzie, J. Magn. Reson. **214**, 144 (2012).
[6] A.N. Garroway, P.K. Grannell and P. Mansfield, J. Phys. C **7**, L457 (1974).
[7] S.R. Giblin, S.P. Cottrell, P.J.C. King, S. Tomlinson, S.J.S. Jago, L.J. Randall, M.J. Roberts, J. Norris, S. Howarth, Q.B. Mutamba, N.J. Rhodes, F.A. Akeroyd, NIM-A, **751**, 70 (2014).

[8] P.E. Spindler, Y. Zhang, B. Endeward, N. Gershernzon, T.E. Skinner, S.J. Glaser, T.F. Prisner, J. Mag. Res. **218**, 49 (2012).
[9] R.R. Ernst, W.A. Anderson, Rev. Sci. Instrum. **37**, 93 (1966).
[10] S.L. Lee, S.H. Kilcoyne, R. Cywinski (Eds.) Muon Science: Muons in Physics, Chemistry and Solids, in: Proceedings of the 50th Scottish University Summer School in Physics, A Nato Advanced Study Institute, vol 51, Institute of Physics, 1998.
[11] F. Casanova and B. Blümich, J. Magn. Reson. **163**, 38-45 (2003).
[12] J.F. Ziegler, M.D. Ziegler, J.P. Biersack, NIM-B **268**, 1818 (2010).
[13] P. Lauterbur, Nature **242**, 190 (1973).
[14] N. Kaplan et al, Hyp. Int. **87**, 1031 (1994).
[15] T. Shiroka et al, NIM-B **152**, 241 (1999).